ELSEVIER

Journal of Structural Geology 29 (2007) 1400–1413

JOURNAL OF STRUCTURAL GEOLOGY

www.elsevier.com/locate/jsg

Formation of tectonic peperites from alkaline magmas intruded into wet sediments in the Beiya area, western Yunnan, China

Xing-Wang Xu [a,*], Xin-Ping Cai [a], Jia-You Zhong [a], Bao-Chang Song [a], Stephen G. Peters [b]

[a] *Key Laboratory of Mineral Resources, Institute of Geology and Geophysics, Chinese Academy of Sciences, Beijing 100029, P.R. China*
[b] *U.S. Geological Survey, Reston, VA 20192, USA*

Received 27 April 2006; received in revised form 24 April 2007; accepted 26 April 2007
Available online 16 May 2007

Abstract

Tertiary (3.78 Ma to 3.65 Ma) biotite-K-feldspar porphyritic bodies intrude Tertiary, poorly consolidated lacustrine sedimentary rocks in the Beiya mineral district in southwestern China. The intrusives are characterized by a microcrystalline and vitreous-cryptocrystalline groundmass, by replacement of some tabular K-feldspar phenocrysts with microcrystalline chlorite and calcite, and by Fe-rich rings surrounding biotite phenocrysts. Peculiar structures, such as contemporary contact faults and slickensides, ductile shear zones and flow folds, foliation and lineations, tension fractures, and banded and boudin peperites, are developed along the contact zones of the intrusives. These features are related to the forceful intrusion of the alkaline magmas into the wet Tertiary sediments. The partially consolidated magmas were deformed and flattened by continued forceful magma intrusion that produced boudinaged and banded peperites. These peperites characterized by containing oriented deformation fabrics are classified as tectonic peperites as a new type of peperite, and formation of these tectonic peperites was related to fracturing of magmas caused by forceful intrusion and shear deformation and to contemporary migration and injection of fluidized sediments along fractures that dismembered the porphyritic magma. Emplacement of the magma into the wet sediments in the Beiya area is interpreted to be related to a large pressure difference rather than to the buoyancy force.

Keywords: Magma; Wet sediments; Intrusion; Tectonic peperites; Beiya; Western Yunnan

1. Introduction

'Peperite', named by Scrope (1858) from the Limagne d'Au-vergne region in central France, is applied to a rock formed essentially in situ by disintegration of magma intruding and mingling with unconsolidated or poorly consolidated, typically wet sediments (White et al., 2000). A number of reports show that intrusion and mingling of magma with wet unconsolidated, or poorly consolidated sediments, are common occurrences (McBirney, 1963; Klein, 1985; Busby-Spera and White, 1987; Branney and Suthren, 1988; Hanson and Wilson, 1993; White, 1996; Goto and McPhie, 1996; Boulter et al., 1999; Hanson and Hargrove, 1999; Doyle, 2000; Skilling et al., 2002). Conditions, processes, and mechanisms of peperite formation are widely discussed and documented (Einsele et al., 1980; Kokelaar, 1982, 1986; Cas and Wright, 1988; Cas, 1992; McPhie et al., 1993). The exsolution of volatiles and growth of bubbles in and around the magma (Kokelaar, 1982, 1986; Cas, 1992), and the difference between the densities of the magma and unconsolidated sediments (Einsele, 1986) are recognized as key elements for peperite formation. In addition, a vesiculation theory discussed by Cashman and Mangan (1994), Mader et al. (1994), and Klug and Cashman (1996) generally is accepted as the mechanism for peperite genesis, but the exact mechanism of intrusion and its influence on peperite formation has not been completely addressed.

We recently discovered some peculiar and interesting deformation structures and peperite along the intrusive contact zones of Tertiary biotite-K-feldspar porphyry bodies that

* Corresponding author. Tel.: +86 10 6200 7331; fax: +86 10 6201 0846.
E-mail addresses: xuxw@mail.igcas.ac.cn (X.-W. Xu), caixp@mail.igcas.ac.cn (X.-P. Cai), speters@usgs.gov (S.G. Peters).

0191-8141/$ - see front matter © 2007 Elsevier Ltd. All rights reserved.
doi:10.1016/j.jsg.2007.04.007

intrude Tertiary poorly consolidated lacustrine sedimentary rocks in Guochanghe in the Beiya mineral district of western Yunnan Province, southwestern China. This paper reports on these deformation structures, and interprets the flow patterns and emplacement mechanism of magma within the wet sediments, and finally hypothesizes on the genesis of the peperite.

2. General geological setting

The Beiya mineral district, 90 km north of Dali in the western Yunnan, is located east of the Jinshajiang suture and shear zone that bounds the western part of Yangtze tectonic plate (Fig. 1a). The Jinshajiang suture forms the line of closure of the Jinshajiang Ocean, a main branch of the Tethys that formed during the Carboniferous between 294 and 340 Ma (Zhang et al., 1985, 1996; Huang and Cheng, 1987; Mo et al., 1993; Wang et al., 2000), and closed during the Late Triassic (Fang, 1993; Zhong et al., 2000; Sun et al., 2002). From Late Cretaceous to Late Tertiary, the Jinshajiang suture was reactivated by subduction and collision of the Indian Plate against the Asian continent (Hou et al., 2003; Guo et al., 2005; Xu et al., 2007), and this produced large thrust and strike-slip

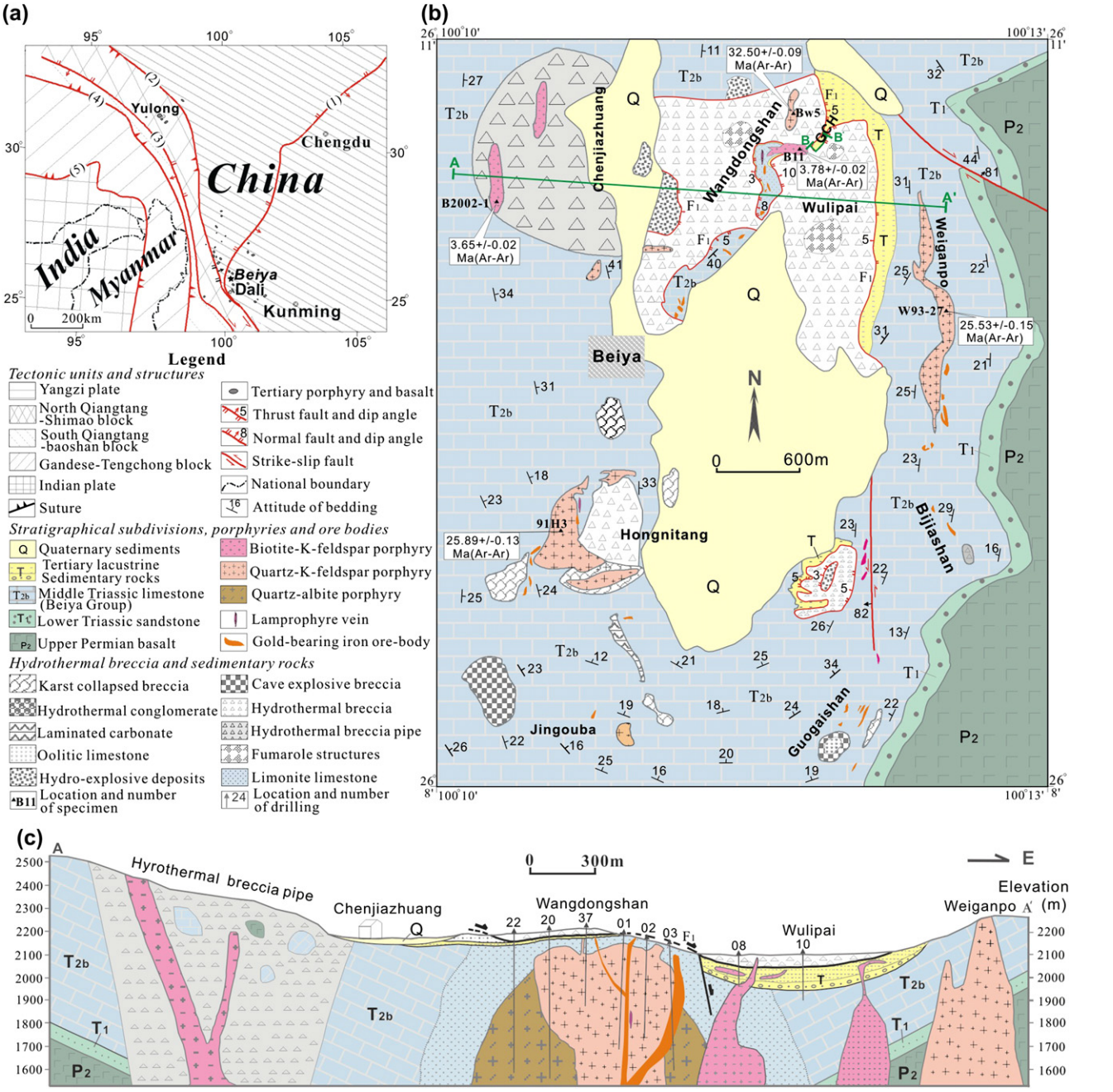

Fig. 1. Tectonic setting (a), geological map (b) and a geological profile A–A′ (c) of the Beiya area, western Yunnan (Revised after Xu et al., 2007). Lines A–A′ and B–B′ in b show location of profile A–A′ in this figure and profile B–B′ in Fig. 3. (1) Rongmenshan thrust fault, (2) Jinshajiang suture, (3) Langchangjian thrust fault, (4) Nujiang suture, (5) Yarlungzangbojiang suture. GCH, Guochanghe. F_1: the fault carrying the hydrothermal breccia sheets in the Wangdongshan, Guochanghe and Wulipai areas.

faults along the suture (Tapponnier et al., 1982; Wang et al., 2000; Gilley et al., 2003; Hou et al., 2003). A great number of alkaline porphyry bodies and volcanic rocks were formed along the Jinshajiang suture and are temporally related to the resubduction of the paleo-Jinshajiang Ocean plate (Liu et al., 2000; Guo et al., 2005; Xu et al., 2007) and to large-scale strike-slip faults (Wang et al., 2001; Zeng et al., 2002; Hou et al., 2003).

Bedrock geology in the Beiya area includes Upper Permian basalt, Lower Triassic sandstone, Middle Triassic limestone, Tertiary lacustrian sedimentary rocks, hydrothermal limestone breccia, and Quaternary sediments (Fig. 1b). The Permian and Triassic strata are present in a north-striking Cenozoic basin upon which is superimposed a broad north-south-elongated synformal basin. The 550 m-thick Middle Triassic Beiya Group limestone is the main ore host rock for the Tertiary porphyry copper-gold deposits (Xu et al., 2007).

The 50- to 200-m-thick Tertiary lacustrian sedimentary rocks are poorly consolidated and unconformably lie over folded limestone of the Beiya Group and some older porphyry bodies (Fig. 1c). These sediments consist of two units: sandstone and conglomerate in the lower parts, and mudstone in the upper parts. Abundant, distinctive quartz-K-feldspar porphyry pebbles, present in the lower parts of the conglomerate indicate that the Cenozoic basin developed after intrusion of the Wangdongshan porphyry. The Tertiary lacustrian sedimentary rocks in Wangdongshan–Wulipai areas were covered by hydrothermally altered limestone breccia.

Tertiary alkaline porphyry plugs are abundant in the Beiya area and include quartz-albite porphyry, quartz-K-feldspar porphyry and biotite-K-feldspar porphyry. Bodies of quartz-albite porphyry are not well-exposed and are detected only at Wangdongshan and Hongnitang by deep drilling (Fig. 1c). The age of the Wangdongshan quartz-albite porphyry is 65.56 ± 0.28 Ma ($^{40}Ar/^{39}Ar$ plateau age of albite) (Xu et al., 2006). The three quartz-K-feldspar porphyritic bodies, at Wangdongshan, Hongnitang, and Weiganpo have intrusive ages of 32.50 ± 0.09 Ma, 25.89 ± 0.13 Ma and 25.53 ± 0.15 Ma ($^{40}Ar/^{39}Ar$ plateau ages of K-feldspar) respectively (Fig. 1b) (Xu et al., 2006). The quartz-albite porphyry was partly intruded and replaced by quartz-K-feldspar porphyry at Wangdongshan (Fig. 1c). Both the quartz-albite porphyry and quartz-K-feldspar porphyry are associated with porphyry Cu–Au and skarn-type polymetallic deposits (Xu et al., 2007).

The biotite-K-feldspar porphyry bodies were intruded into hydrothermal breccia pipes in the Chengjiazhuang area, sucrose-textured limestone in the Wangdongshan area, and lacustrine sedimentary rocks in the Guochanghe and Wulipai area. Some biotite-K-feldspar porphyry bodies were emplaced at higher level near ground surface in the poorly consolidated lacustrine sedimentary rocks. Two biotite-K-feldspar porphyry bodies from Chenjiazhuang and Wangdongshan (sample

Table 1
Summary of argon isotopic results[a]

Temp. °C	$(^{40}Ar/^{39}Ar)m$	$(^{36}Ar/^{39}Ar)m$	$(^{37}Ar/^{39}Ar)m$	$(^{38}Ar/^{39}Ar)m$	$^{39}Ar_k$	$(^{40}Ar^*/^{39}Ar_k)$	$^{39}Ar_k$	Age ± 1σ
					10^{-12} mol	±1σ	%	Ma
B11 biotite ($J = 0.00813$, $W = 0.1105$ g)								
400	8.2268	0.0191	1.2269	0.30990	7.255	2.685 ± 0.030	2.81	38.97 ± 1.28
500	5.2255	0.0124	0.63136	0.16640	14.91	1.600 ± 0.016	5.78	23.33 ± 0.47
600	3.4588	0.0100	0.42963	0.12349	23.10	0.5198 ± 0.011	8.96	7.61 ± 0.13
700	4.6849	0.0149	0.18652	0.0869	23.19	0.2639 ± 0.007	9.00	3.87 ± 0.06
800	3.1618	0.0098	0.12050	0.04797	40.13	0.2536 ± 0.003	15.5	3.72 ± 0.05
900	2.3533	0.0070	0.11243	0.03462	65.65	0.2550 ± 0.002	25.4	3.74 ± 0.05
1000	2.4781	0.0074	0.15772	0.0356	37.11	0.2560 ± 0.002	14.4	3.75 ± 0.05
1130	2.6576	0.0081	0.20758	0.0396	25.74	0.2610 ± 0.003	9.99	3.83 ± 0.05
1280	4.0781	0.0129	0.29144	0.0500	14.84	0.2590 ± 0.004	5.76	3.80 ± 0.05
1420	8.2661	0.0262	0.59727	0.11088	5.751	0.5818 ± 0.010	2.23	8.52 ± 0.13
B2002-1 biotite ($J = 0.00847$, $W = 0.1201$ g)								
420	8.1400	0.0195	0.23423	0.12866	7.121	2.418 ± 0.2653	0.771	32.27 ± 8.5
540	7.5581	0.0211	0.22604	0.09090	10.970	1.361 ± 0.2286	1.18	18.24 ± 4.16
660	4.1904	0.0129	0.20223	0.07253	17.900	0.3987 ± 0.070	1.94	5.36 ± 0.38
740	3.2222	0.0101	0.17394	0.06490	22.960	0.2666 ± 0.041	2.48	3.59 ± 0.16
820	3.0312	0.0093	0.14045	0.06010	29.690	0.2861 ± 0.037	3.21	3.85 ± 0.15
860	1.2336	0.0032	0.04070	0.01823	113.200	0.2699 ± 0.006	12.2	3.63 ± 0.05
900	1.4562	0.0040	0.05760	0.02460	74.230	0.2640 ± 0.0086	8.04	3.55 ± 0.05
950	1.0108	0.0024	0.02770	0.01290	213.400	0.2747 ± 0.004	23.1	3.70 ± 0.05
1000	1.0827	0.0027	0.03910	0.01770	134.500	0.2719 ± 0.004	14.5	3.66 ± 0.05
1060	1.3037	0.0035	0.04380	0.02090	125.200	0.2700 ± 0.006	13.5	3.63 ± 0.05
1140	1.0213	0.0025	0.04650	0.01940	108.500	0.2685 ± 0.004	11.7	3.61 ± 0.05
1220	2.1124	0.0062	0.08870	0.03060	37.110	0.2797 ± 0.017	4.02	3.76 ± 0.08
1300	3.2125	0.0099	0.10644	0.04370	18.550	0.2792 ± 0.041	2.01	3.76 ± 0.16
1400	5.8762	0.0167	0.17070	0.07470	9.000	0.9646 ± 0.1382	0.975	12.95 ± 1.79

[a] Argon isotope analyses were conducted on an RGA-10 mass spectrometer in the Laboratory of Isotope Geochronology at the Institute of Geology and Geophysics, Chinese Academy of Sciences (IGCAS). Age calculations were made using the decay constants given by Steiger and Jäger (1977), and the formulations of Wang et al. (1985) and Wang (1992).

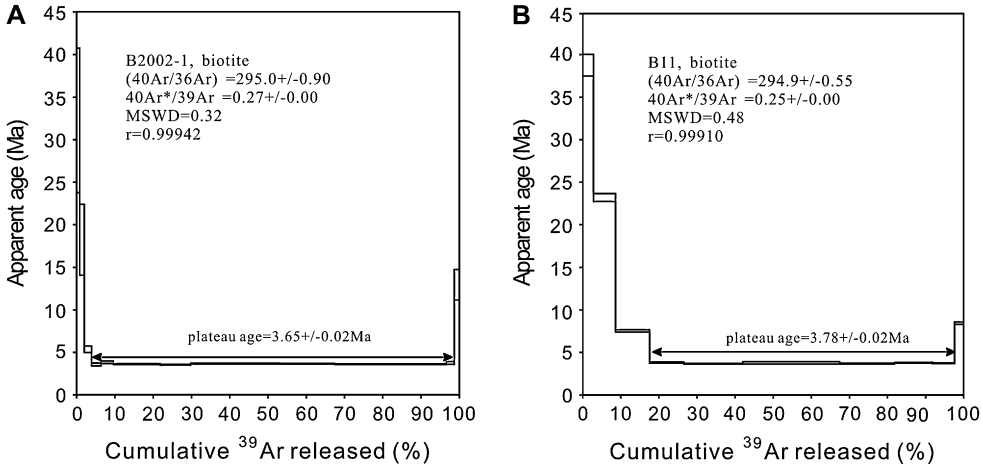

Fig. 2. $^{40}Ar/^{39}Ar$ plateau ages of biotite from the biotite K-feldspar porphyry in Chenjiazhuang (A) and Wangdongshan (B).

B2002-1 and B11) are dated about 3.65 ± 0.02 Ma and 3.78 ± 0.02 Ma respectively (Table 1, Figs. 1b and 2).

Karst formation and hydrothermal brecciation in the Beiya Group limestone produced karst collapse breccia, hydrothermal karst conglomerate, laminated carbonate, hydrothermal explosive deposits, fumarolic hydrothermal breccia sheets and hydrothermal breccia pipes (Fig. 1b) (Xu et al., 2003a). The fumarolic hydrothermal breccia sheets overlay Tertiary lacustrian sedimentary rocks in the Wangdongshan and Wulipai areas and slid *en-masse* or were ejected from the hydrothermal breccia pipe at Chenjiazhuang (Xu et al., 2003a).

Development of the Cenozoic basin involved normal faults and some small, steep-dipping, strike-slip faults in the Beiya area. All these structures are related to the India-Asia collision, and the region has been deforming since the India-Asia collision started to the present.

3. Features of the biotite-K-feldspar porphyry in the poorly consolidated lacustrine sedimentary rocks

Most biotite-K-feldspar porphyry bodies that intrude the poorly consolidated lacustrine sedimentary rocks are tabular and <10 m in length, but larger bodies are 0.5 to 3 m thick, 1 to 5 m wide, and 5 to 20 m long, and occur as tubes or pipes (Figs. 3 and 4a,b). Smaller porphyry bodies are irregular veins (Fig. 4c,d). Some tube-shaped porphyry bodies cut bedding planes in the sedimentary host rocks (Fig. 4a), but the irregular porphyry veins invade fractures and bedding planes (Fig. 4d).

The biotite-K-feldspar porphyry bodies have both aphanitic and porphyritic hypabyssal textures. The outer contact zones contain well-developed fluidal structures, present as oriented biotite and vitreous breccia (Fig. 5a). Cores of the porphyry bodies contain both microcrystalline and vitreous-cryptocrystalline groundmasses (Fig. 5b). In addition, some tabular K-feldspar phenocrysts were replaced by microcrystalline chlorite (Fig. 5c) and calcite (Fig. 5d). Occurrences of Fe-rich biotite rings (Fig. 5c) suggest that Fe-rich water was added into the porphyritic magma system during the crystallization process and that these replacements were related to magma-water interaction. These textures indicate that the magmas were only partially crystallized when they were intruded into the wet sediments and are compatible with waters from the wet host sediments that were added to and mixed with the biotite-K-feldspar porphyry magmas during emplacement.

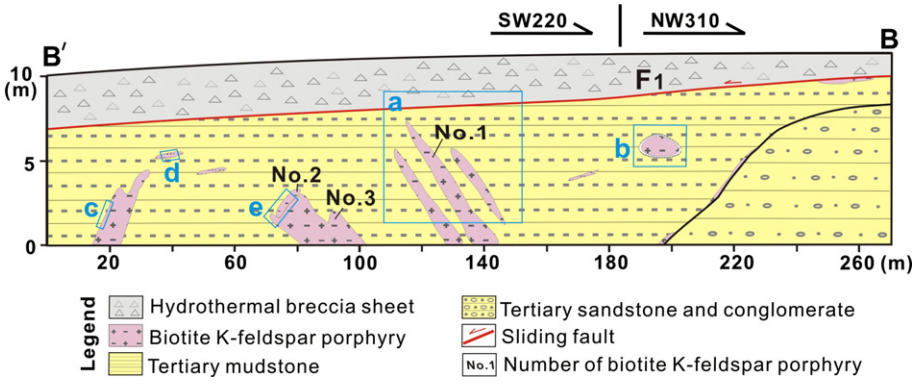

Fig. 3. A geological profile B–B′ of the southern cliff to the Guochanghe valley showing distribution of the biotite K-feldspar porphyries in the poorly consolidated lacustrine sedimentary rocks at Guochanghe (see Fig. 1b for location). The rectangles a, b, c, d and e show locations of picture a and b in Fig. 4, two pictures in Fig. 6, picture in Fig. 7, and picture a in Fig. 11, respectively.

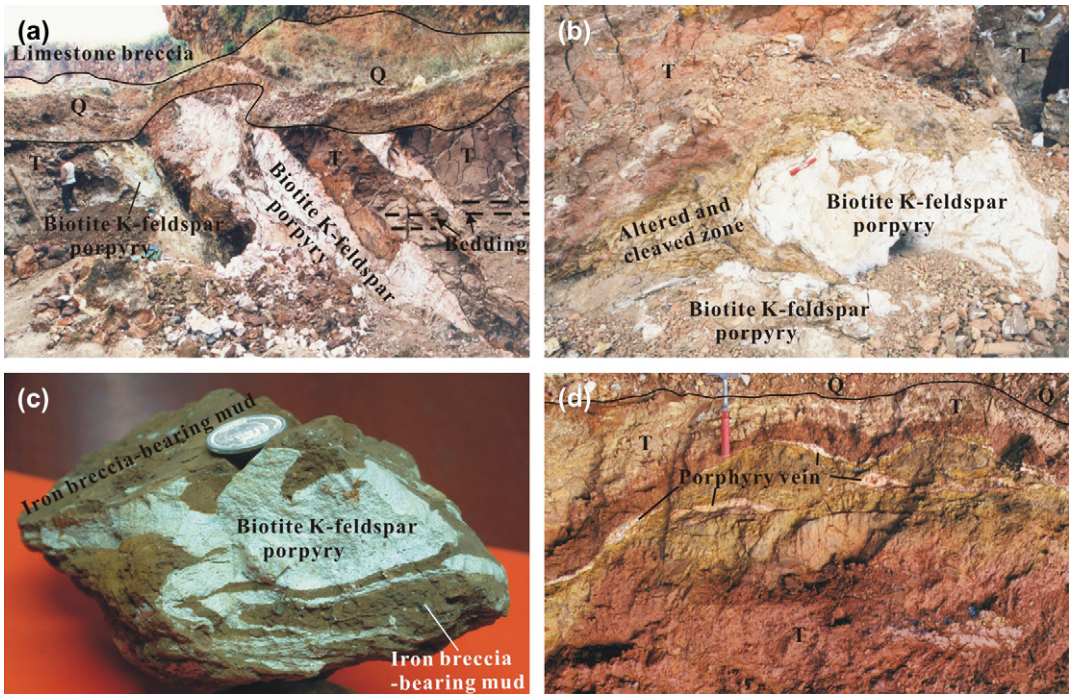

Fig. 4. Photographs showing shapes and distribution of the biotite K-feldspar porphyry in the poorly consolidated lacustrine sedimentary rocks at Guochanghe. (a) Tube like biotite K-feldspar porphyritic bodies cut through the bedding of host sedimentary rocks. The man is about 165 cm tall. Q, Quaternary. Location of this picture is shown in Fig. 3 by rectangle a. (b) A tube-shaped biotite K-feldspar porphyritic body intruded and compressed host sedimentary rocks to produce a rounded ring-like altered and cleaved zones. T, Tertiary. The marker pen is 14 cm long. Location of this picture is shown in Fig. 3 by rectangle b. (c) Irregular biotite K-feldspar porphyritic veins in Fe-rich, breccia-bearing mud. The coin diameter is 2 cm. (d) Fine porphyritic veins present along fractures and lithostratigraphic interfaces. T, Tertiary; Q, Quaternary. The hammer is 30 cm long.

4. Deformational structures associated with the biotite K-feldspar porphyry in the lacustrine sedimentary rocks

Structures associated with biotite-K-feldspar porphyry in lacustrine sedimentary rocks consist of contact faults and slickensides, ductile shear zones, flow folds, foliation and lineations, boudinage and compressive fractures, and peperites. Development and distribution of these structures are related to the size and shape of the individual biotite-K-feldspar porphyritic bodies. All these deformation structures described and discussed below are observed on the southern cliff to the Guochanghe valley (Figs. 1b and 3).

4.1. Contact fault, slickenside, fractures and peperites

The common and well-developed contact faults along the smooth sided contacts of the biotite-K-feldspar porphyry bodies form in contact zones, which contain slip planes, slickenside lineations, and step-shaped fissures. The shape of these contact zones is related to that of the biotite-K-feldspar porphyries, such that many of the pipe-shaped biotite-K-feldspar porphyry bodies contain pipe-shaped contact zones (Fig. 6).

Some contact zones contain a series of slip planes with concentrated slickenside lineations and steps along the contact fault, with perpendicular fractures filled by clay with some sand grains smaller than that in their host sedimentary rocks At an outcrop of the contact fault of the No. 4 biotite K-feldspar porphyry, the contact fault consists of more than five smooth, slip planes and a 2-cm-wide fault gouge zone with each gouge layer separated by 2- to 5-mm-thick slip planes. In these cases, slickenside lineations are present on the small offset slip planes and plunge parallel to trend of the contact fault plane (Fig. 7a). Here, the clay-filled fractures are ‘‘V’’-shaped in cross-section with the wide parts connecting to the fault plane, and net-like textures on the porphyry-sediment boundary. Such features can be divided into wide and narrow types. The wide fractures are about 2 to 3 cm wide and 5 to 6 cm deep. The narrow fractures are less than 1 cm wide and about 4 to 5 cm deep and parallel or oblique to the slickenside lineations. The narrow fractures crosscut each other and are cut through by the wider fractures (Fig. 7b). These clay-filled fractures dismembered the biotite-K-feldspar porphyry, and net-like textures along the contacts as the peperite formed.

In some cases, slickenside lineations on the contact fault planes of small pipe-shaped porphyritic bodies may also have ring-like shapes and be oblique to the contact (Fig. 6). Commonly these features are contained in a red gibbsite and limonite membrane or crust that transitions into the porphyry along complex fissure planes (Fig. 6).

4.2. Banded peperites and ductile shear structures

Banded peperite consists of bands of porphyry rock and poorly consolidated sedimentary rock. Sub types of banded

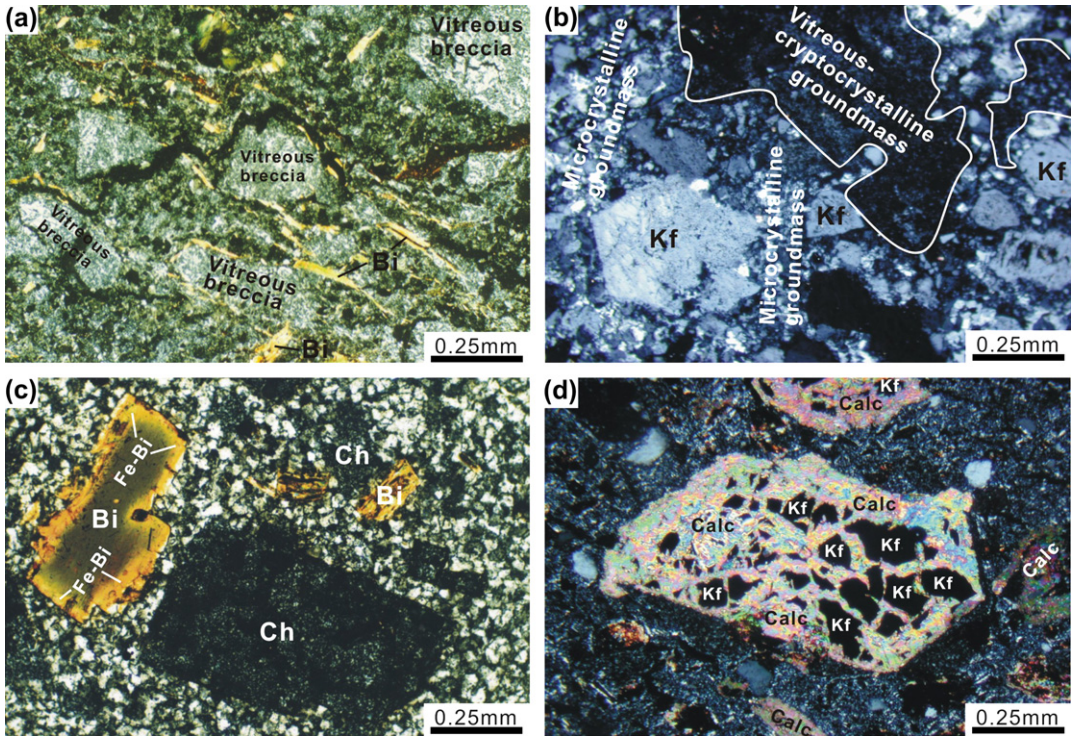

Fig. 5. Microphotographs showing textures of the biotite K-feldspar porphyry in the poorly consolidated lacustrine sedimentary rocks at Guochanghe. (a) Biotite (Bi) and vitreous breccia are oriented and produced fluidal structures. (b) Coexistence of microcrystalline groundmass and vitreous-cryptocrystalline groundmass in porphyry. Kf, K-feldspar. (c) Tabular K-feldspar phenocrysts are replaced by microcrystalline chlorite, and Fe-rich biotite rings formed along the outer rims of a biotite phenocryst. Ch, chlorite; Fe-Bi, Fe-rich biotite. (d) Tabular K-feldspar phenocrysts were replaced by calcite with many relicts. Calc, calcite; Kf, K-feldspar.

peperite are present as lenticular, folded, and S-C pattern shapes. Various banded peperites regularly surround many biotite-K-feldspar porphyritic bodies and contain different textures and structures.

At Guochanghe, the lenticular, folded, and S-C patterned, and banded peperites are developed along the top, front, and bottom respectively of the contact zone between the 2-m-wide, >8-m-long No. 1 irregular-shaped biotite-K-feldspar porphyry, which dips 45° to 50° south, and the poorly consolidated lacustrine sedimentary rocks (Figs. 8 and 9a).

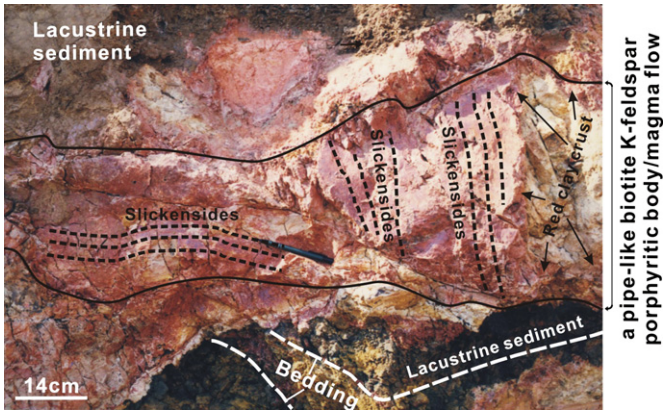

Fig. 6. Photograph showing a pipe-like biotite K-feldspar porphyry body with ring-like and oblique slickensides on its outside surface (fault plane) and a 5-cm-thick red clay crust in the poorly consolidated lacustrine sedimentary rocks at Guochanghe. The change between the red clay crust and the inner porphyry is gradual. Location of this picture is shown in Fig. 3 by rectangle c.

Lenticular banded peperites are 10 cm wide, 50 cm long lenticular bodies that have sharp contacts with the country rocks consisting of a 1-cm-thick clay membrane (Fig. 9b). They consist of bands of white biotite-K-feldspar porphyry (<50 volume percent) and orange-yellow clay without sand grains (Fig. 9c). The 2-cm-long, 0.5-cm-wide, evenly distributed porphyritic bands are platy and lenticular and are oriented vertically, but are oblique at a angle of about 45° to the contact between the platy peperites and sedimentary host (Fig. 9b). The porphyritic bands in the lenticular banded peperites constitute more than 50 volume percent of the rock, but decrease from the foot wall to the hanging wall of the contact. Both the hanging wall and foot wall contacts of the lenticular banded peperites are contact faults (slip planes) and contain slickensides and step-shaped fissures indicating right-hand shearing. Commonly, there is a 2-mm-thick clay membrane between the lenticular-banded peperites and the sedimentary host.

Folded banded peperites are present as flame-like shapes adjacent to the biotite-K-feldspar porphyry (Fig. 9d). They consist of folded interbeds of <1-cm-thick, brown clay bands, brown clay-bearing porphyritic rocks, and white porphyritic rocks. Both the brown and white porphyritic rocks are foliated with penetrative lineations along the foliation. The folded banded peperites also contain small, well-developed sheath and Z-type folds (Fig. 9e).

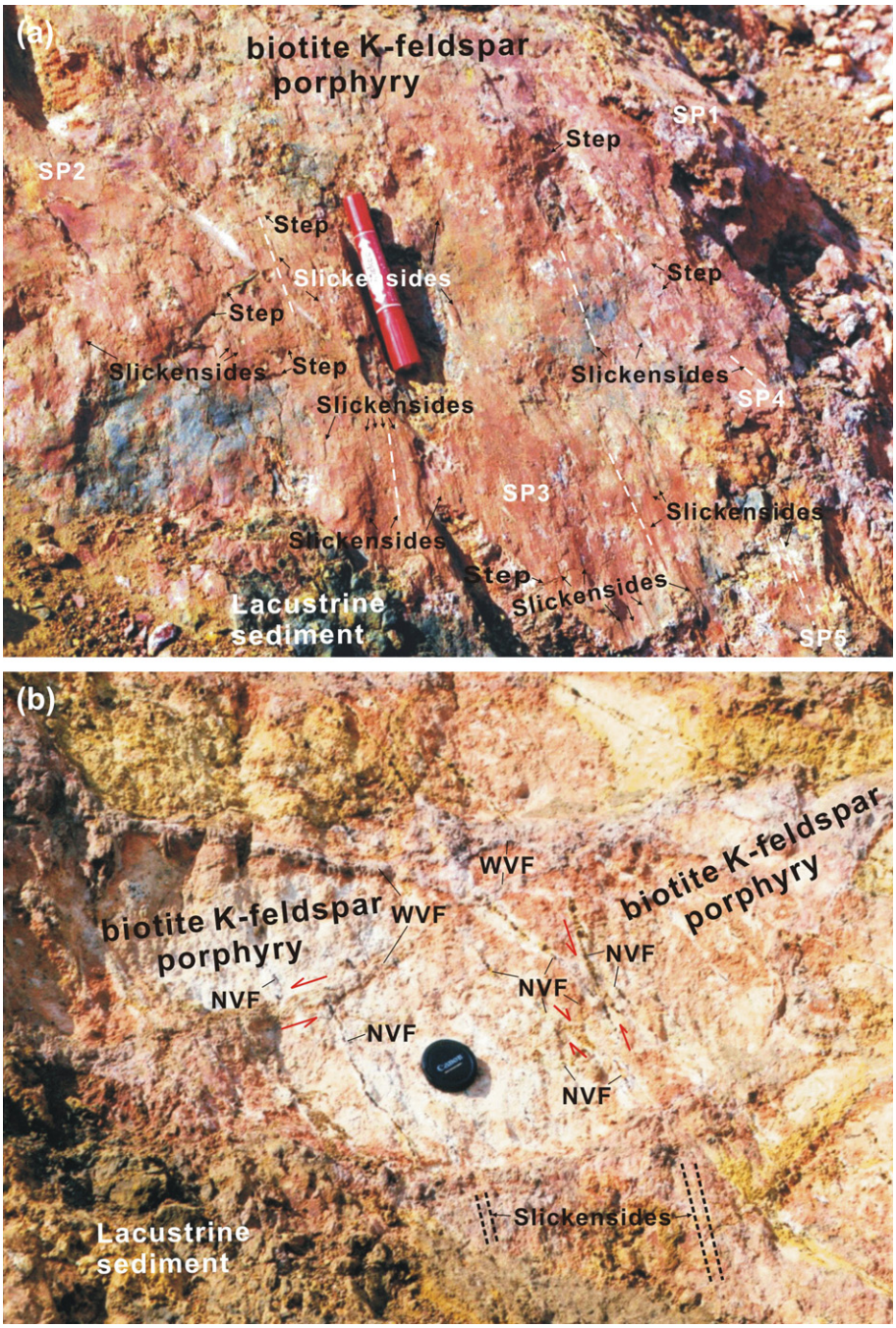

Fig. 7. Photographs showing a contact fault with a series of slip planes (SP), concentrated slickenside lineations and steps (a) and sediment-filled "V"-type fractures in the biotite K-feldspar porphyritic body under the contact fault (b) in Guochanghe. NVF, narrow "V"-type fracture; SP1, 2, 3, 4, 5, slip plane number 1, 2, 3, 4, 5 respectively; WVF, wider "V"-type fracture. Dashed lines in image a show the trend of the slickenside lineations on slip planes. The marker pen is 14 cm long, and the lens is 6 cm in diameter. Locations of these two pictures are shown in Fig. 3 by rectangle d.

The S-C pattern banded peperites are about 15 to 20 cm wide and more than 120 cm long and have sharp and irregular contacts with the sedimentary rocks (Fig. 9f). They consist of bands of brown clay and white porphyritic rocks with bands arranged in S-C patterns at small angles (less than 30°) oblique to the contact (shear zone boundary) with the sedimentary host (Fig. 9g). The proportion of clay bands decreases from the contact face to the inner part of the porphyry. The porphyritic bands are foliated with penetrative lineations on the foliation. Textures and structures of the banded peperites both at macro and micro scales contain S-C symmetries (Fig. 9g,h). The clay bands in the S-C pattern banded peperites generally are <30 volume percent.

Clay bands in the three kinds of banded peperite are characterized lack of sand grains, whereas their adjacent host sedimentary rocks contain some sand grains and 2-mm in diameter breccia zones. All three banded peperite subtypes show ductile shear deformation. The S-C pattern banded

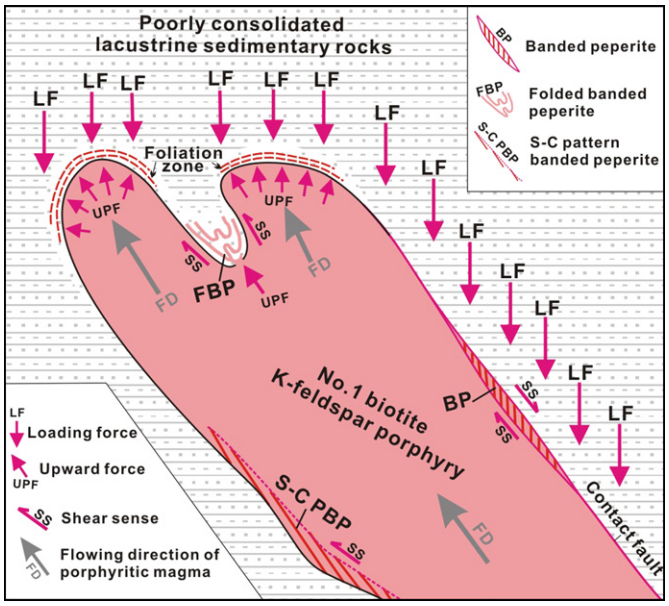

Fig. 8. Schematic section through the No. 1 BKFP showing distribution of three various banded peperites and their dynamic formation model of the banded peperites associated to the No. 1 magma flow at Guochanghe. Location of No. 1 BKFP is shown in Fig. 3.

peperites are typical of ductile shear zones, whereas the folded banded peperites are present as shear folds.

4.3. Boudin peperites and compressive structures

Boudinaged peperites, consisting of boudin-shaped porphyry rocks and poorly consolidated sedimentary rocks, are present in about 30-cm-wide and 1.8-m-long bodies of the tube-shaped No. 2 K-feldspar porphyry, in the lacustrine sedimentary rocks at Guochanghe, where the entire porphyritic body consists of boudinaged and banded peperite (Fig. 10a).

The boudinaged peperites can be subdivided into lenticular, rectangular, and fish-shaped boudinaged peperite according to shape of the porphyritic boudins (Fig. 10b). The 0.5- to 20-cm-long lenticular porphyritic boudins are mainly boudin shape with length to width ratios from 3:2 to 4:1 and some contain short narrow tails. The rectangular boudins (Rectangular boudin-1, shown in Fig. 10b) formed over lenticular boudins, which makes their two side surfaces saw-toothed shaped and nearly perpendicular to the trend of parent porphyritic boudin. Fine-grained 0.2- to 2-cm-thick sediment may be present between adjacent rectangular boudins. Rectangular and fish-shaped boudins mainly are present in the hanging wall of the No. 2 peperite bodies, whereas most lenticular boudin peperites lie in middle of the No. 2 peperite. All rectangular, lenticular, and fish-shaped porphyritic boudins are parallel to the elongation of their parent porphyry body and most rectangular and lenticular porphyritic boudins are symmetric (Fig. 10).

The banded peperites lie in the foot wall of the No. 2 peperite bodies as closely packed, porphyritic bands that are parallel to the elongation of their parent porphyry body. The banded peperites have been deformed to Z-type folds at the ends of the No. 2 peperite body.

Sediments located between rectangular porphyritic boudins usually contain sand grains and small breccia zones, whereas these sand grains and small breccia zones are absent in clay bands in lenticular and banded peperites.

Some peperite bodies (Fig. 10a) contain small faults (fault F_{10} and F_2, in Fig. 10a; fault F_3 in Fig. 10b). These faults are normal and developed over the boudinaged and banded peperite rocks. For example, fault F_{10} and F_2, along the right limb of the No. 2 peperite, are normal strike faults developed along the contact between the lenticular boudinage peperite and the banded peperite and they penetrate and truncate the contact zone within the banded peperite (Fig. 10a). In addition, there is a variable normal separation across fault F_3, the dislocation distance of the rectangular boudin-1 (point A to point A′) is larger than that of the lenticular boudin LB-1 (point B to point B′), and distance between of the rectangular boudin-1 and the lenticular boudin-1 on hanging wall of the fault F_3 is shortened (Fig. 10a).

5. Formation mechanisms of the deformation structures and peperites associated with biotite K-feldspar porphyry in the lacustrine sedimentary rocks

5.1. Genesis of the deformation structures and peperites

Deformation structures and peperite described above are only present along contacts of some biotite-K-feldspar porphyries which did not intrude along faults, and the host lacustrine sedimentary rocks; specifically, those rocks above and near the apices of the porphyries were not affected by fault and shear deformation. This indicates that the genesis of these deformation structures and peperites are directly related to intrusion of the porphyry bodies into the lacustrine sediments, instead of being related to regional tectonic deformation. This also implies that the contact faults, ductile shear zones and compressive structures associated with the peperites also are related to intrusion and mixing of the magma with the wet sediments.

The observation that slickenside lineations are coplanar with their host contact fault planes or foliation is compatible with the hypothesis that the contact faults and ductile shear zones are related to the uprising and movement of magma into wet sediments. Development of ring-shaped and oblique slickenside lineations (Fig. 6) strongly suggests that flow movement of pipe-shaped magma in the unconsolidated lacustrine sedimentary rocks was forceful and helical. Occurrence of red membranes or crust along complex fault planes within the contact zone (Figs. 6 and 7a) suggests that the porphyritic magmas were altered along the complex, faulted contact zone during or shortly after intrusion.

5.2. Formation mechanism of tectonic peperites

Features of the banded and boudin peperites containing oriented deformation fabrics indicate that peperite in the Beiya area originated from tectonic stress directly related to forceful magmatic intrusion. This mechanism differs from other peperite genesis induced by steam explosion or by quench

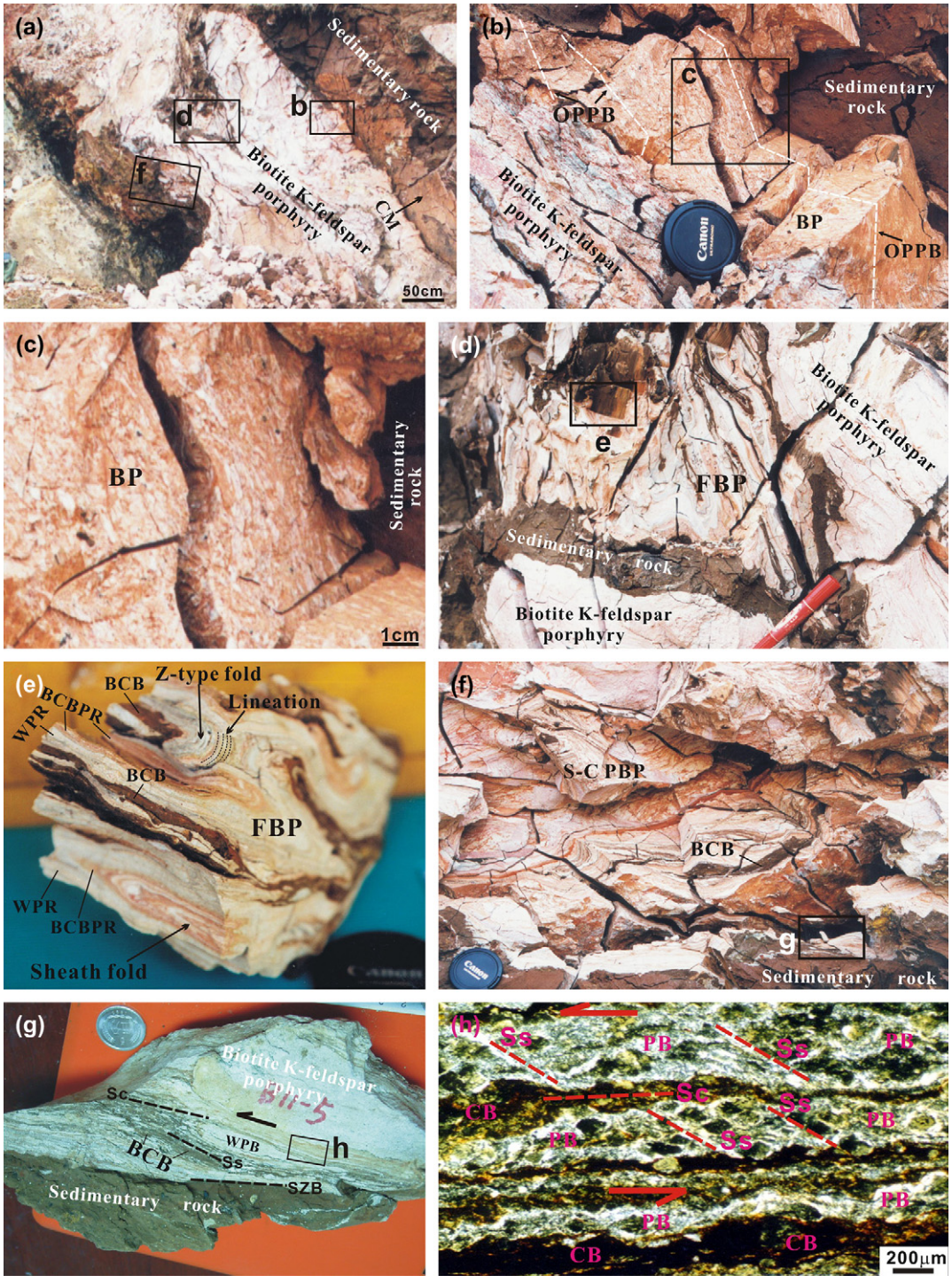

Fig. 9. Photographs and microphotograph showing distribution, texture and structure of peperites associated with the No. 1 biotite K-feldspar porphyritic body in the poorly consolidated lacustrine sedimentary rocks at Guochanghe. (a) Shape of the No. 1 biotite K-feldspar porphyry. CM, clay membrane. The three black rectangles show locations of picture b, d and f. (b) Banded peperites (BP). The white broken lines show oriented plane of porphyritic bands (OPPB). The lens is 6 cm in diameter. The black rectangle shows location and area of picture c. (c) Enlargement of the banded peperites in picture b. (d) Folded banded peperites (FBP). The marker pen is 14 cm long. The black rectangle shows location of the specimen in picture d. (e) A specimen of folded banded peperites (FBP). The lens is 6 cm in diameter. (f) S-C pattern banded peperites (S-C PBP). The marker pen is 14 cm long. The black rectangle shows location of the specimen in picture g. (g) A specimen of S-C pattern banded peperites (S-C PBP). Sc, shear bands parallel to shear zone boundary; Ss, main foliation oblique to shear zone boundary; SZB, shear zone boundary; WPB, white porphyry band. The coin is 2 cm in diameter. BCB, brown clay band. The black rectangle shows location of thin section P11-3. (h) Banded peperites in micro-scale in a thinner section P11-3. CB, clay band; PB, porphyry band; Sc, shear bands parallel to shear zone boundary; Ss, main foliation oblique to shear zone boundary.

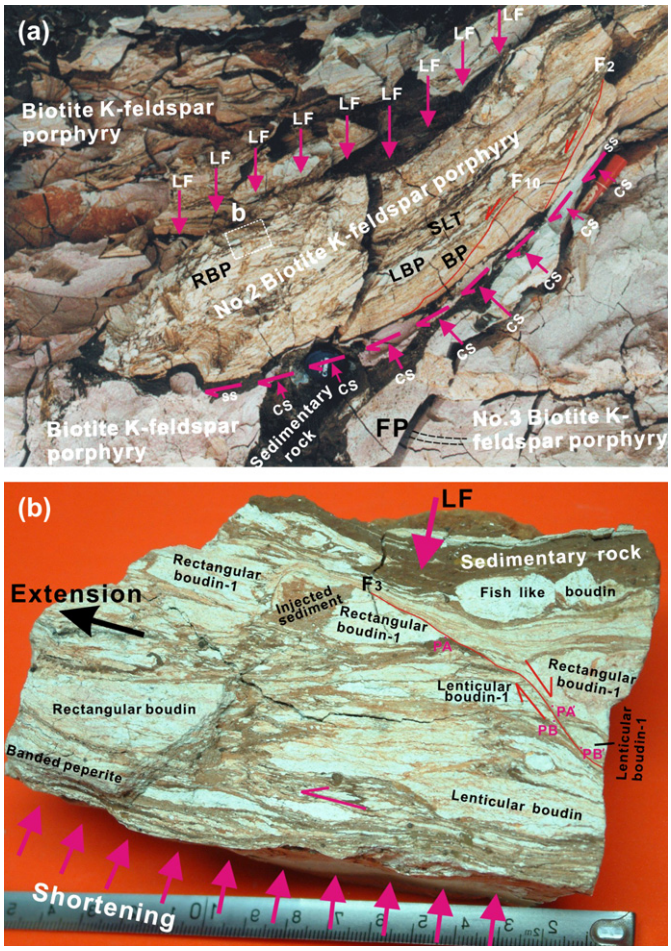

Fig. 10. Photographs showing shape (a) and inner texture and structure and (b) their dynamic origin of the No. 2 peperite body at Guochanghe. F_1, F_2 and F_3, number of the fault; CS, compressive stress; BP, banded peperites; FP, fluidal plane; LBP, lenticular boudin peperites; LF, loading force; RBP, rectangular boudin peperites; PF, pushing force; SLT, strip-like tail; SS, shear stress. Location of picture a is shown in Fig. 3 by rectangle e.

fragmentation described in the literature by Fisher (1960), Kokelaar (1982, 1986); Cas (1992), Hanson and Wilson (1993), Goto and McPhie (1996), Hanson and Hargrove (1999), Skilling et al. (2002), and Wohletz (2002). We therefore suggest the term *tectonic peperite* as a new classification of peperite. Key questions regarding the formation mechanism of the tectonic peperites are: How did sediment-filled fractures form?; how did sediment migrate into the fractures?; and why did intensive shear deformation take place between the emplacing porphyritic magma and their unconsolidated country sedimentary rock?

5.2.1. Formation mechanism of net-like peperites

Narrow clay-filled "V"-type fractures cross cut each other and also cut through by wider clay-filled "V"-type fractures (Fig. 6b). This is consistent with multistage deformation and clay filling, and a reasonable interpretation is that the narrow "V"-type fracture networks were related to quenching of the magma as it touched the cooler wet sediment. The wider "V"-type fractures may have been enhanced as extension fractures grew due to shear deformation at the contact fault as magma flowed through the sediment. Evidence that clays in these fractures and net-like peperites contain fine sand grains that are smaller in size than in their host sedimentary rocks suggests that the poorly consolidated host sedimentary rocks had been fluidized at along the magma-sediment contact zones, producing clay flows containing smaller sand grains that were injected into the fractures along with the clay.

5.2.2. Formation mechanism of the banded peperite associated with the No. 1 biotite-K-feldspar porphyry

Formation of lenticular and S-C pattern banded peperites associated with the No. 1 biotite-K-feldspar porphyry is interpreted to be related to shear deformation between magma and poorly consolidated sediment, which resulted in injection of fluidized sediment into shear fractures within the partially crystallized porphyritic magma along its margins.

Because clay bands in the banded peperite lack sand grains it is likely that only very fine-grained clay particles migrated and were extracted from the fluidized host sediments, which contain some sand grains and breccia at the contact zone, into contemporary fractures within the adjacent porphyritic magmas.

Microstructures within S-C pattern banded peperite contain clay bands that are distributed along foliation layers and separate the foliated porphyritic rocks to form porphyritic bands. The density and thickness of the clay bands decrease away from the porphyry-sediment contact to the inner parts of the porphyry (Fig. 11), which is compatible with fluidized sediment and fine-grained, clast-loaded water migration along shear planes and foliation. During this migration shear deformation was ductile with left-hand shear sense, and the deforming magmas behaved as a plastic. The observations that the distribution pattern of the clay bands and structure of the clay bands share the same shearing pattern and shear sense to that of the foliated planes in the porphyry strongly suggests that injection of sediment was synchronous with deformation. After the magma consolidated and fine-grain clasts (clay) were deposited, clay bands formed as the porphyritic rocks were dismembered, leading to the formation of the S-C pattern banded peperite.

Formation of the lenticular banded peperites is also related to similar shear deformation to that of the S-C pattern peperites. Since the angle between the oriented vertical porphyritic bands and the contact fault planes is about 45°, the right-hand shear sense along the hanging wall and foot wall boundaries of the lenticular banded peperite implies that the fractures most likely opened along the shear faces of bands in the porphyritic rocks and were injected with clay from the clay membrane. This is a similar mechanism to the fluidized wet sediment entering secondary shear fractures of contact faults, produced in an experiment by Ma et al. (1994) and also to those reported by Schulson (2004) in arctic sea ice fractures. Orientation and distribution of porphyritic bands in the banded peperite are therefore likely the result of injections of fluidized clay that disrupted the magmas to form banded peperites and that this process was probably synchronous with the formation of

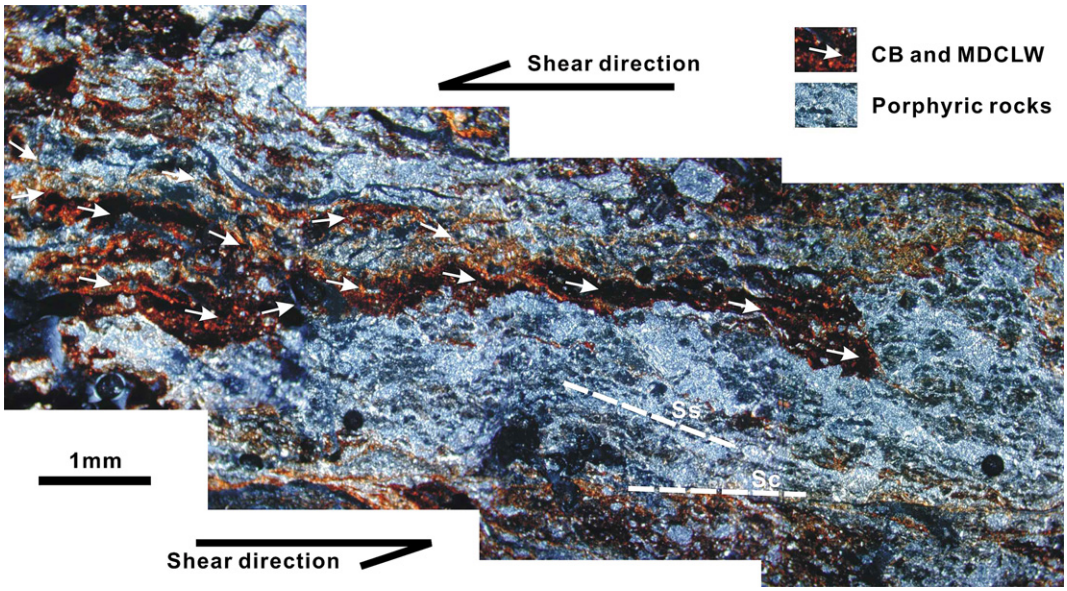

Fig. 11. Microphotograph showing ductile shear deformation and formational mechanism of a clay band in the S-C pattern banded peperites associated with the No. 1 biotite K-feldspar porphyry at Guochanghe. CB, clay band; MDCLW, migrating direction of clast-loaded water; Sc, shear bands parallel to shear zone boundary; Ss, main foliation oblique to shear zone boundary. Sample P11-3 location is shown in Fig. 9g.

the shear fractures. Since the shear deformation that produced the banded peperite was brittle-ductile, the lenticular-banded peperites represent rocks formed in a brittle-ductile zone.

Both the hanging wall brittle-ductile and the foot wall ductile shear zones resulted from shear stress caused by differential flow and from movement along the margins of the intruding porphyry during magma flow (Fig. 8). Deformation of folded banded peperite was caused by an upward force and by shear stress that was due to forceful intrusion of the magma. The upward force produced a foliation zone (FZ) along the apical contact zone of the magma (Fig. 3b), because intrusion of the magma produced differential movement between the outer border of the contact zones and the inner magma. This differential movement further produced shear stress and caused the contacts of the magma to deform as brittle-ductile and ductile shear zones that produced the banded peperites. This upward force also caused the magma contact zone to mingle with the sedimentary bands and simultaneously to fold them towards the tops of the cupola (Fig. 8).

5.2.3. Formation mechanism of the No. 2 boudinage peperite

Boudin structures in the No. 2 peperite bodies are similar to boudins observed in ductile deformation zones, such as that Jiaoluotage ductile compressional zone in the eastern Tianshan Mountains (Xu et al., 2003b). The difference in these two regimes is that the fine-grained material (clay) surrounding the Beiya boudin and lenses are foreign, implying that their formation is most likely due to tectonic stress associated with injections of fluidized clay from the sediment along fractures. Therefore, the porphyry would have been ductile and plastic as partly crystallized magma when these peperites formed. The clay may also locally have acted as fault gouge as the softer rocks moved around hardened rectangular boudinaged blocks of porphyry.

Occurrences of symmetric rectangular and lenticular porphyritic boudins parallel to the elongation of the parent porphyry body (Fig. 10b) indicate that the in the porphyritic body some compressive stress was perpendicular to the elongation of the porphyritic body so that the body was flattened and elongated. The Z-fold symmetry of the banded peperite on the foot wall contacts of the porphyry indicates right-hand shear deformation due to shear stress from below. Because bands of porphyry rock broke off the main body at its margins to form rectangular boudin, such the rectangular boudin-1 showed in Fig. 10b, the property of the intrusive body during intrusion is interpreted to have changed progressively from first ductile and then to partly consolidated magma flow, culminating in ductile-brittle deformation of the margins of the porphyritic rocks during the deformation and consolidation process. Shear and compressive stress along the foot wall surface were due to compression caused by the forceful upward intrusion of the No. 3 biotite K-feldspar porphyry body below the No. 2 biotite K-feldspar porphyry body (Fig. 10a). Weak bending in the No. 2 peperite body and normal faults are may be related to progressive deformation of the No. 2 peperite body caused by the overloading force and the force from the No. 3 porphyritic body.

Evidence that sediments located between rectangular porphyritic boudins usually contain sand grains and little breccia, and that the clay bands in lenticular and banded peperites are devoid of sand grains and breccia indicates that migration of fluidized sediments also experienced two stages: migration of fine clay separated from the fluidized sediments into fractures of magmas, and injection of fluidized sediments with sand grains and breccia into some tensile fractures of partly consolidated porphyritic rocks at its hanging wall margin.

5.3. Emplacement of porphyritic magmas and driving force for forceful intrusion of the magmas in the lacustrine sedimentary rocks in the Beiya area

Shear deformation is evident between the porphyritic magmas and their country sedimentary rocks, but the effect of the No. 3 porphyritic magmas on the No. 2 partly consolidated sediment and formation of peperite is related to the property of the sediments and to the corresponding driving forces for the rising magma.

Characteristics of the Beiya peperite indicate that large volumes of fine-grained sediment migrated along fractures that were produced by intensive shear deformation. This shear deformation is interpreted to be related to the upward forceful intrusion along the margins of the intruding magmas but may also have been due to tectonic forces that dismembered the partly consolidated magmas to form the tectonic peperite. This is consistent with the sediment being poorly consolidated or unconsolidated during the alkaline magma intrusive event. Wet, unconsolidated sediment is easier for magmas to intrude and to rise into and emplace than consolidated rock.

5.3.1. Emplacement pattern of the magmas intruded in the wet sediments

The biotite-K-feldspar porphyry that was intruded into the poorly consolidated sedimentary rocks forms small tube- or pipe-shaped bodies rather than mushroom-shaped bodies. The intrusive contacts also lack shatter breccia and blocks from the host rocks lying in the porphyry. Similarly, deformation of country rocks adjacent to most porphyries elsewhere is weak, indicating that emplacement of the porphyritic magmas at Beiya is different from textbook emplacement models of magma, that are usually characterized by diapirism, ballooning (Ramsay, 1989), and stoping, and therefore pulsed, single event intrusion of the Beiya biotite-K-feldspar porphyritic magmas was directly affected by the poorly consolidated host rocks into which it intruded.

The presence of contact faults with slickenside lineations and steps, contact brittle-ductile and ductile shear zones, and fold structures associated with the banded peperites along the contact zones, and the occurrence of tube or pipe like shapes of the intrusive bodies indicate that emplacement of the magmas into the wet sediments was forceful.

5.3.2. Driving force for the magmas to move up and intrude

The driving force for magma ascent and emplacement is often assumed to be buoyancy (Berner et al., 1972; Marsh, 1982; Spence et al., 1987; Takada, 1989; Lister and Kerr, 1991; Clemens and Mawer, 1992; Petford et al., 1993; Clemens et al., 1997). Buoyancy models hypothesize the rise and intrusion of magmas in the crust to be due to the buoyancy force, which is caused by the lesser density of the magma compared to that of the surrounding rocks (Foster, 1983). The buoyancy model, however, does not operate well for intrusions of the Beiya biotite-K-feldspar porphyry into the poorly consolidated lacustrine sedimentary rocks.

Density data for alkaline magma and wet unconsolidated sediments is difficult to precisely quantify for the time that the Beiya biotite-K-feldspar porphyry magma was intruded; however, densities can be estimated by measuring the densities of the existing biotite-K-feldspar porphyry and sedimentary rocks in the Beiya area. Results of this estimation show that the density of the alkaline magma is about 2210 kg/m^3 ($\pm$50) for 12 specimens from the Beiya area, based on the assumption that the density of magma is about 90 percent of the density of the equivalent solid rock. Similarly, the density of the wet unconsolidated sediments is $<$1900 kg/m^3 according to the measured values between 1660 kg/m^3 and 1900 kg/m^3 for 10 Beiya specimens with an error of $<$1%. These estimates imply that the magma was heavier than the wet sediments and therefore, the buoyancy force was not operating on the alkaline magmas as they invaded the wet sediments. Moreover, oblique and horizontal intrusion of magma into wet sediments, as shown in Figs. 3, 4 and 7, also indicates that the force causing the magma to be intruded was not the buoyancy force, because the buoyancy force dictates that less dense material will have an upward fluid movement.

Ascent of the magmas in shallow levels of the crust in the Beiya area was caused by movement of the magma under high pressure from its chamber below into pre-existing faults, fractures and karst openings above. Some fault conduits may have been connected to the lower pressure surface or subsurface. The magma movement was driven by the pressure difference between the high pressure magma and the low pressure in the fractures and fault. This large pressure differential allowed the magma velocity to accelerate as it passed through and along the pre-existing faults and fractures, similar to injection of basalt magmatic pulses into soft sediments reported by Einsele (1986). Remaining questions concerning mechanisms of recharge of the high pressure magma chamber and propagation of fractures connecting the magma chamber to the overlying pre-existing fractures and faults are worthy of further study.

6. Conclusions

Peperites associated with the Tertiary biotite-K-feldspar porphyries in the Beiya area are characterized by containing oriented deformation fabrics and classified as tectonic peperites as a new type of peperite. Formation of these tectonic peperites in the Beiya area was the result of fracturing of magmas caused by dynamic intrusion and shearing deformation of the sedimentary host interface and contemporary migration and injection of fluidized sediments along fractures that dismembered the porphyritic magmas.

The forceful intrusion and flow of the Tertiary alkaline magmas in the Tertiary wet sediments in the Beiya area produced coeval faults with slickenside lineations along the contact zones, and also caused the magma to deform and produce ductile shear zones, flow folds and tectonic banded peperites along the hybrid contact. The partially consolidated magmas were deformed and flattened and produced boudin and banded peperites by continuing forceful magma intrusion.

Forceful emplacement of the magma into the wet sediments is interpreted from field and laboratory evidence to be the result of acceleration of magma movement due to pressure differences between the magma and the overlying faults and fractures in the host sediments.

Acknowledgments

This study is supported by the National Natural Science Foundation of China (Grant numbers 40272090 and 40572131), the National 973 project of China (Grant number 2002CB412605), and the cooperated research project set by Yunnan Province (Grant number Yk98008-1). We would like to express our gratitude to Jiliang Li, Dongxun Li, Yucheng Cai, Zhengqian Hou, Kaihui Yang, Weiguang Yang, Pusheng Zheng, Rongfu Pei, Jie Wang, Baolin Zhang, Baochang Song, Yonggui Zhao and Kezhang Qin for valuable suggestions and discussions. The paper was significantly improved by the thorough and incisive review of Lawrence J. Drew, Charles G. Cunningham, Thomas G. Blenkinsop, James D.L. White and an anonymous reviewer.

References

Berner, H., Ramberg, H., Stephansson, O., 1972. Diapirism in theory and experiment. Tectonophysics 15, 197–218.

Branney, M., Suthren, R., 1988. High-level peperitic sills in the English Lake District: distinction from block lavas, and implications for Borrow dale Volcanic Group stratigraphy. Geological Journal 23, 171–187.

Boulter, C.A, Wilton, V.M., Cox, D.J., 1999. Magma-wet-sediment interaction: The most widespread yet least recognized alteration system in the Iberian pyrite belt (A). In: Stanley, C.J. (Ed), Mineral deposits: processes to processing (volume1) (C), A.A.BALKEMA, London, 483–486.

Busby-Spera, C.J., White, J.D.L., 1987. Variation in peperite textures associated with differing host-sediment properties. Bulletin of Volcanology 49, 765–775.

Cashman, K.V., Mangan, M.T., 1994. Physical aspects of magmatic degassing II. Constraints on vesiculation processes from textural studies of eruptive products. In: Carroll, M.R., Holloway, J.R. (Eds.), Volatiles in Magmas. Reviews in Mineralogy, 30, pp. 447–478.

Cas, R.A.F., 1992. Submarine volcanism: eruption styles, products and relevance to understanding the host-rock successions to volcanic-hosted massive sulfide deposits. Economic Geology 87, 511–541.

Cas, R.A.F., Wright, J.V., 1988. Volcanic Successions—Modern and Ancient. Unwin Hyman, London. 54-5543–46.

Clemens, J.D., Mawer, C.K., 1992. Granitic magma transport by fracture propagation. Tectonophysics 204, 339–360.

Clemens, J.D., Petford, N., Mawer, C.K., 1997. Ascent mechanisms of granitic magmas: causes and consequences. In: Holness, M.B. (Ed.), Deformation-Enhanced Fluid Transport in the Earth's Crust and Mantle. Chapman & Hall, London, pp. 144–171.

Doyle, M.G., 2000. Clast shape and textural associations in peperite as a guide to hydromagmatic interactions: Upper Permian basaltic and basaltic andesite examples from Kaman, Australia. Australian Journal of Earth Sciences 47, 167–177.

Einsele, G., 1986. Interaction between sediments and basalt injections in young Gulf of California-type spreading centers. Geologische Rundschau 75, 197–208.

Einsele, G., Gieskes, J.M., Curray, J., Moore, D., Aguayo, E., Aubry, M.P., Fornari, D.J., Guerrero, J.C., Kastner, M., Kelts, K., Lyle, M., Matoba, Y., Molina-Cruz, A., Niemitz, J., Rueda, J., Saunders, A., Schrader, H., Simoneit, B., Vacquier, V., 1980. Intrusion of basaltic sills into highly porous sediments, and resulting hydrothermal activity. Nature 283, 441–445.

Fang, N., 1993. View of the closure of the Palaeo-Tethys: evidence from post Permian pelagic sedimentary records in western Yunnan. In: Wang, H. (Ed.), Accretion of the Asia. Seismological Publishing House, Beijing, pp. 57–60.

Fisher, R.V., 1960. Classification of volcanic Breccias. Geological Society of America Bulletin 71, 973–982.

Foster, R.J., 1983. Physical geology. Charles E. Merrill Publishing, Columbus. p61–63.

Gilley, L.D., Harrison, T.M., Leloup, P.H., Ryerson, F.J., Lovera, O.M., Wang, J., 2003. Direct dating of left-lateral deformation along the Red River shear zone, China and Vietnam. Journal of Geophysical Research 108 (B2), 2127, doi:10.1029/2001JB001726.

Goto, Y., McPhie, J., 1996. A Miocene basanite peperitic dyke at Stanley, northwestern Tasmania, Australia. Journal of Volcanology and Geothermal Research 74 (1-2), 111–120.

Guo, Z.F., Hertogen, J., Liu, J.Q., Pasteels, P., Boven, A., Punzalan, L., He, H.Y., Luo, X.J., Zhang, W.H., 2005. Potassic magmatism in western Sichuan and Yunnan provinces, SE Tibet, China: Petrological and geochemical constraints on petrogenesis. Journal of Petrology 46 (1), 33–78.

Hanson, R.E., Hargrove, U.S., 1999. Processes of magma/wet sediment interaction in a large-scale Jurassic andesitic peperite complex, northern Sierra Nevada, California. Bulletin of Volcanology 60, 610–626.

Hanson, R.E., Wilson, T.J., 1993. Large scale rhyolitic peperites (Jurassic, southern Chile). Journal of Volcanology and Geothermal Research 54, 247–264.

Hou, Z., Ma, H., Zhang, Y., Wang, M., Wang, Z., Pan, G., Tang, R., 2003. The Hinalayan Yulong porphyry Cu belt: Product of large-scale strike-slip faulting in eastern Tibet. Economic Geology 18, 125–145.

Huang, J., Cheng, B., 1987. The Evolution of the Tethys in China and Adjacent Region. Seismological Publishing House, Beijing, 109 pp.

Klein, G.D., 1985. The control of depositional depth, tectonic uplift and volcanism on sedimentation processes in the back-arc basins of the western Pacific Ocean. Journal of Geology 93, 1–25.

Klug, C., Cashman, K.V., 1996. Permeability development in vesiculating magmas: implications for fragmentation. Bulletin of Volcanology 58, 87–100.

Kokelaar, B.P., 1982. Fluidization of wet sediments during the emplacement and cooling of various igneous bodies. Journal of the Geological Society of London 139, 21–33.

Kokelaar, B.P., 1986. Magma-water interactions in subaqueous and emergent basaltic volcanism. Bulletin of Volcanology 48, 275–289.

Lister, J.R., Kerr, R.C., 1991. Fluid-mechanical models of crack propagation and their application to magma transport in dikes. Journal of Geophysical Research 96, 10049–10077.

Liu, F., Liu, J., He, J., You, Q., 2000. A subduction slab of Yangtze block under Tethys orogenic belt, western Yunnan. Chinese Science Bulletin 45, 79–83. in Chinese.

Ma, Z.J., Zhong, J.Y., Li, T., 1994. Properties of deflection conjugated shear fault of the Hexi System structure, in: Geomechanics and Crust Movement—Annual Report of the Laboratory of Geomechanics, Ministry of Geology and Mineral Resource, RPC. Seismic Publishing House, Beijing, p. 1–10 (in Chinese with English abstract).

Mader, H.M., Zhang, Y., Phillips, J.C., Sparks, R.S.J., Sturtevant, B., Stolper, E., 1994. Experimental simulations of explosive degassing of magma. Nature 372, 85–88.

Marsh, B.D., 1982. On the mechanics of igneous diapirism, stoping, and zone melting. American Journal of Science 282, 808–855.

McBirney, A.R., 1963. Factors governing the nature of submarine volcanism. Bulletin of Volcanology 26, 455–469.

McPhie, J., Doyle, M., Allen, R., 1993. Volcanic Textures: A Guide to the Interpretation of Textures in Volcanic Rocks. University of Tasmania, Centre for Ore Deposit and Exploration Studies, Launceston, TAS, Australia. p57–58.

Mo, X., Lu, F., Shen, S., 1993. Sanjiang Tethyan Volcanism and Related Mineralisation. Geological Publishing House, Beijing, 267 pp. (in Chinese with English abstract).

Petford, N., Kerr, R.C., Lister, J.R., 1993. Dike transport of granitoid magmas. Geology 21, 845–848.

Ramsay, J.G., 1989. Emplacement kinematics of a granite diapir: the Chindamara batholith, Zimbabwe. Journal of Structural Geology 11, 191–209.

Scrope, G.P., 1858. The Geology and Extinct Volcanoes of Central France. John Murray, London, 258 pp.

Schulson, E.M., 2004. Compressive shear faults within arctic ice: Fracture on scale large and small. Journal of Geophysical Research 109, C07016, doi:10.1029/2003JC002108.

Skilling, I., White, J.D.L., McPhie, J., 2002. Peperite: a review of magma-sediment mingling. Journal of Volcanology and Geothermal Research 114, 1–17.

Spence, D.A., Sharp, P.W., Turcotte, D.L., 1987. Buoyancy-driven crack propagation: A mechanism for magma migration. Journal of Fluid Mechanics 174, 135–153.

Steiger, R.H., Jäger, E., 1977. Subcommission on geochronology: convention on the use of decay constants in geo- and cosmochronology. Earth and Planetary Science Letters 36, 359–362.

Sun, Y., Chen, L., Feng, T., Gao, M., He, Y., 2002. A dynamic model of Palaeo-Tethyan evolution: evidences from Palaeo- Tethyan ophiolite in China. Journal of Northwest University (Natural Science Edition) 32, 1–6.

Tapponnier, P., Pelter, G., Armijo, G., Le, Dain, 1982. Propagating extrusion tectonics in Asia: new insight from simple experiments with plasticine. Geology 10, 611–616.

Takada, A., 1989. Magma transport and reservoir formation by a system of propagating cracks. Bulletin of Volcanology 52, 118–126.

Wang, S., 1992. Constraints of chlorine on $^{40}Ar/^{39}Ar$ dating and calculation of high-precise $^{40}Ar/^{39}Ar$ ages. Scientia Geologica Sinica 27, 369–378 (in Chinese with English abstract).

Wang, S., Sang, H., Hu, S., 1985. $^{40}Ar/^{39}Ar$ age determinant using 49-2 reactor and $^{40}Ar/^{39}Ar$ age spectrum for amphibolite from Qianan, China. Acta Petrologica Sinica 2, 35–44 (in Chinese with English abstract).

Wang, P.-L., Lo, C.-H., Chung, S.-L., Lee, T.-Y., Lan, C.-Y., Yem, N.T., 2000. Onset of the movement along the Ailao Shan-Red River Shear Zone: evidence from $^{40}Ar/^{39}Ar$ thermochronogical data. Journal of Asian Earth Sciences 18, 281–292.

Wang, J.H., Yin, A., Harrison, T.M., Grove, M., Zhang, Y.Q., Xie, G.H., 2001. A tectonic model for Cenozoic igneous activities in the eastern Indo-Asian collision zone. Earth and Planetary Science Letters 188, 123–133.

White, J.D.L., 1996. Impure coolants and interaction dynamics of phreatomagmatic eruptions. Journal of Volcanology and Geothermal Research 74, 155–170.

White, J.D.L., McPhie, J., Skilling, I., 2000. Peperite: a useful genetic term. Bulletin of Volcanology 62, 65–66.

Wohletz, K., 2002. Water/magma interaction: some theory and experiments on peperite formation. Journal of Volcanology and Geothermal Research 114, 19–35.

Xu, X.W., Cai, X.P., Xiao, Q.B., Liang, G.H., Zhang, B.L., 2003a. Hydrothermal Karst and their associated geological disasters in the Beiya area, western Yunnan province. Advance in Earth Sciences 18, 897–905 (In Chinese with English abstract).

Xu, X.W., Ma, T.L., Sun, L.Q., Cai, X.P., 2003b. Characteristics and dynamic origin of the large-scale Jiaoluotage ductile compressional zone in the eastern Tianshan Mountains, China. Journal of Structural Geology 25, 1901–1915.

Xu, X.W., Cai, X.P., Song, B.C., Zhang, B.L., Ying, H.R., Xiao, Q.B., Wang, J., 2006. Petrologic, chronological and geochemistry characteristics and formation mechanism of alkaline porphyries in the Beiya gold district, western Yunnan. Acta Petrologica Sinica 22, 631–642 (In Chinese with English abstract).

Xu, X.W., Cai, X.P., Xiao, Q.B., Peters, S.G., 2007. Porphyry Cu-Au and associated polymetallic Fe-Cu-Au deposits in the Beiya Area, Western Yunnan Province, South China. Ore Geology Reviews 31, 224–246.

Zeng, P.-S., Mo, X., Yu, X.-H., 2002. Nd, Sr and Pb isotopic characteristics of the alkaline-rich porphyries in western Yunnan and its compression strike-slip setting. Acta Petrologica et Mineralogica 21, 231–241 (in Chinese with English abstract).

Zhang, Q., Li, D., Zhang, K., 1985. Preliminary study on Tongchangjie ophiolite mélange from Yun county, Yunnan Province. Acta Petrologica Sinica 1, 1–4 (in Chinese with English abstract).

Zhang, Q., Zhou, D., Chen, Y., 1996. A new type oceanic crust and its dynamic significance. Chinese Science Bulletin 41, 25–27. in Chinese.

Zhong, D., Ding, L., Liu, F., Liu, J., Zhang, J., Ji, J., Chen, H., 2000. Multi-directional bedding-form structures of lithosphere in orogenic belt and its constraint to Cenozoic magmatic activity - for example in Sanjiang and its adjacent area. Science in China 30 (supplement) 1-8. (in Chinese).